and control, enabling real-time optimization of the bioprocess operation. These approaches are obviously complementary to one another. This book discusses the matter within the context of the final approach.

1.2. Specific problems of bioprocess control

Over the past several decades, biotechnological processes have been increasingly used industrially, which is attributed to several reasons (improvement of profitability and quality in production industries, new legislative standards in processing industries, etc.). The problems arising from this industrialization are generally the same as those encountered in any processing industry and we face, in the field of bioprocessing, almost all of the problems that are being tackled in automatic control. Thus, system requirements for supervision, control and monitoring of the processes in order to optimize operation or detect malfunctions are on the increase. However, in reality, very few installations are provided with such systems. Two principal reasons explain this situation:

– first of all, biological processes are complex processes involving living organisms whose characteristics are, by nature, very difficult to apprehend. In fact, the modeling of these systems faces two major difficulties. On the one hand, lack of reproducibility of experiments and inaccuracy of measurements result not only in one or several difficulties related to selection of model structure but also in difficulties related to the concepts of structural and practical identifiability at the time of identification of a set of given parameters. On the other hand, difficulties also occur at the time of the validation phase of these models whose sets of parameters could have precisely evolved over course of time. These variations can be the consequence of metabolic changes of biomass or even genetic modifications that could not be foreseen and observed from a macroscopic point of view;

– the second major difficulty is the almost systematic absence of sensors providing access to measurements necessary to know the internal functioning of biological processes. The majority of the key variables associated with these systems (concentration of biomass, substrates and products) can be measured only using analyzers on a laboratory scale – where they exist – which are generally very expensive and often require heavy and expensive maintenance. Thus, the majority of the control strategies used in industries are very often limited to indirect control of fermentation processes by control loops of the environmental variables such as dissolved oxygen concentration, temperature, pH, etc.

1.3. A schematic view of monitoring and control of a bioprocess

Use of a computer to monitor and control a biological process is represented schematically in Figure 1.1. In the situation outlined, the actuator is the feed rate of the reactor. Its value is the output of the control algorithm, which uses the information of the available process. This information regroups, on the one hand, the state

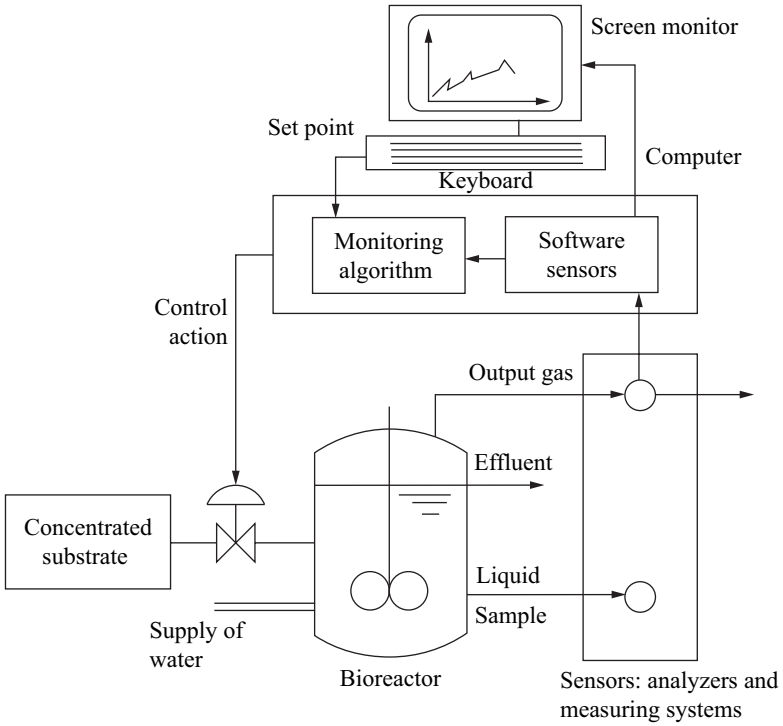

Figure 1.1. *Schematic representation of bioprocess control system*

of the process to date (i.e. measurements) and, on the other hand, available *a priori* knowledge (for example, in the form of a "material balance" model type) relative to a dynamic biological process and mutual interactions of different process variables. In certain cases – and in particular, when control objectives directly use variables that could not be measured (certain concentrations of biomass, substrates and/or products) or key parameters of the biological process (growth rate or more generally production rate, yield coefficients, transfer parameters) – information resulting from "in-line" measurements and *a priori* knowledge will be combined to synthesize "software sensors" or "observers," whose principles and methods will be presented in Chapters 4 and 5. Thus, according to the available process knowledge and control objectives specified by the user, we will be able to develop and implement more or less complex control algorithms.

1.4. Modeling and identification of bioprocesses: some key ideas

The dynamic model concept plays a central role in automatic control. It is in fact on the basis of the time required for the development of the knowledge process that

the total design, analysis and implementation of monitoring and control methods are carried out. Within the framework of bioprocesses, the most natural way to determine the models that will enable the characterization of the process dynamics is to consider the material balance (and possibly energy) of major components of the process. It is this approach that we will consider in this work (although certain elements of hybrid modeling, which combines balance equations and neural networks, will be addressed in the chapter on modeling). One of the important aspects of the balance models is that they consist of two types of terms representing, respectively, conversion (i.e. kinetics of various biochemical reactions of the process and conversion yields of various substrates in terms of biomass and products) and the dynamics of transport (which regroups transit of matter within the process in solid, liquid or gaseous form and the transfer phenomena between phases). These models have various properties, which can prove to be interesting for the design of monitoring and control algorithms for bioprocesses, and which will, thus, be reviewed in Chapter 2. Moreover, we will introduce in Chapter 4 on state observers a state transformation that makes it possible to write part of the bioprocess equations in a form independent of the process kinetics. This transformation is largely related to the concept of reaction invariants, which are well known in the literature in chemistry and chemical engineering.

An important stage of modeling consists not only of choosing a model suitable and appropriate for describing the bioprocess dynamics studied but also of calibrating the parameters of this model. This stage is far from being understood and therefore no solution has been obtained, given the complexity of models as well as the (frequent) lack of sufficiently numerous and reliable experimental data. Chapter 3 will attempt to introduce the problem of identification of the parameters of the models of the bioprocess (in dealing with questions of structural and practical identifiability as well as experiment design for its identification) and suitable methods to carry out this identification.

1.5. Software sensors: tools for bioprocess monitoring

As noted above, sometimes many important variables of the process are not accessible to be measured online. Similarly, many parameters remain unclear and/or are likely to vary with time. There is, thus, a fundamental need to develop a model, which makes it possible to carry out a real-time follow-up of variables and key parameters of the bioprocess. Thus, Chapters 4 and 5 will attempt, respectively, to develop software tools to rebuild the evolution of these parameters and variables in the course of time. Insofar as their design gives reliable values to these parameters and variables, they play the role of sensors and will thus be called “software sensors”. The material is divided between the two chapters on the basis of distinction between state variables (i.e. primarily, component concentrations) whose evolution in time is described by differential equations and parameters (kinetic, conversion and transfer parameters), which are either the functions of process variables (as is typically the case for kinetic parameters

such as specific growth rates) or constants (output parameters, transfer parameters)[1]. For state variables, we will proceed with the design of "software sensors" called state observers (Chapter 4), whereas for estimating the unknown or unclear parameters online, parameter estimators will be used (Chapter 5). Due to space considerations, Chapter 5 will deal exclusively with the estimation of kinetic parameters, which proves to be a more crucial problem to be solved. However, the methods which are developed are also applicable to other parameters.

1.6. Bioprocess control: basic concepts and advanced control

An important aspect of bioprocess control is to lay down a stable real time operation, less susceptible to various disturbances, close to a certain state or desired profile compatible with an optimal operating condition. Chapter 6 will attempt to develop the basic concepts of automatic control applied to bioprocesses, particularly the concepts of control and setpoint tracking, feedback, feedforward control and proportional and integral actions. We can also initiate certain control methods specific to bioprocesses. The following chapter will concentrate on the development of more sophisticated control methods with the objective of guaranteeing the best possible bioprocess operation while accounting, in particular, for disturbances and modeling uncertainties. Emphasis will be placed, particularly, on optimal control and adaptive control methods based on the balance model as developed in the chapter on modeling. The objective is clearly to obtain control laws, which seek the best compromise between what is well known in bioprocess dynamics (for example, the reaction scheme and the material balance) and what is less understood (for example, the kinetics).

1.7. Bioprocess monitoring: the central issue

With the exception of real-time monitoring of state variables and parameters, there has been little consideration of bioprocess monitoring. In particular, how to manage bioprocesses with respect to various operation problems, which are about malfunctioning or broken down sensors, actuators (valves, pumps, agitators, etc.), or even more basically malfunction of the bioprocess itself, if it starts to deviate from the nominal state (let us not forget that the process implements living organisms, which can possibly undergo certain, at least partial, transformations or changes, which are likely to bring the process to a different state from that expected). This issue is obviously important and cannot be ignored if we wish to guarantee a good real time process operation. This problem calls for all the process information (which is obtained from modeling, physical and software sensors or control). This will be covered in the final chapter.

---

1. The models used in practice are often so simplified with respect to reality that these parameters can "apparently" undergo certain variations with time. However, it is important to note that these variations are nothing but a reflection of the inaccuracy or inadequacy of the selected model.

for its robustness with respect to the local minima, its ease of implementation and its reasonable convergence speed [PRE 86, SCH 98, VAN 96].

Global minimization

The global minimization methods can be roughly classified into two groups [SCH 98]. The first group comprises purely deterministic methods, such as the gridding method. It consists of evaluating the objective function for a large number of points predefined over a grid covering the parameter space. If there is a sufficient number of function evaluations, there are chances of attaining the minima. This method is not very effective, unless it is improved by refining the grid after a series of evaluations.

The second group of global methods can be called random probing methods, as random decisions are included in the procedure for attaining the optimum. Among them, the adaptive methods take into account the information obtained during the preceding evaluations. For one method (simulated annealing [PRE 86]), the idea is that the search will not always be toward a possible solution (which could just be a local minimum), but may be, from time to time, along another direction. This method can be viewed as preceding the popular methods such as genetic algorithms (GA) [GOL 89]. These algorithms commence with an initial population of prospective solutions (somewhat similar to the edges in the Simplex method) sampled in a random manner in the parameter space. In genetic algorithms, new prospective solutions are obtained by imitating the process of biological evolution of cross breeding, mutation and selection among the parameter "populations". The definition of the parameters of the algorithm itself is crucial for correct implementation.

3.6. A case study: identification of parameters for a process modeled for anaerobic digestion

The anaerobic digestion model (2.16)–(2.29) formed the subject matter for a systematic study to identify parameters on the basis of a fixed bed reactor of LBE - INRA at Narbonne (see [BER 01, BER 00] for a more detailed study). This case study is remarkable in view of many aspects. Firstly, the identification of parameters is riddled with traps that are typical for biological systems: the process is very complex (numerous bacterial populations participate in the process; they can have different behaviors depending on the operating conditions). There are no direct measurements for each of the acidogenic and methanogenic bacterial populations and in general, a limited number of process variables are accessible. The process is slow and can be destabilized easily by the accumulation of fatty acids. These characteristics have significant consequences for the selected model. The model cannot be very complex lest it should turn out to be non-identifiable, whereas the simplified modeling hypotheses can have an impact on its capacity to predict the dynamics of the process. The choice of the structure is therefore a critical stage in view of the fact that the model should necessarily contain elements that are essential for the process dynamics.

Moreover, the identification itself contains original elements with respect to the rest of the chapter. Constraints on the process have led us to conceive an experimental plan, not on the basis of the above techniques but motivated by concern for covering as wide a range of operating conditions as possible, while at the same time limiting the duration (here necessarily long) of the experiments as much as possible. In addition, the structure of the reaction system models enables us to separate the parameters into three classes (yield coefficients, kinetic parameters and transfer parameters) and to carry out the identification of each class of parameters in a distinct manner.

In this case study, emphasis is laid on parameter estimation using linear regression. Having said this, it will be prudent to draw attention to the fact that this approach cannot turn out to be optimum from a statistical point of view insofar as the statistical conditions on the variables used in the linear regression could not be completely fulfilled in order to enable an estimation that might be statistically accurate and sufficiently reliable. In general, care must be taken during the interpretation of the estimated values of parameters and their standard deviation. Furthermore, these parameter values given by linear regression were suggested to be used as initial values of an estimation on the basis of the nonlinear model. However, such an estimation has not turned out to be useful in the present case.

3.6.1. *The model*

Let us once again proceed from the equations developed in Chapter 2. A variant of these was considered as here we are dealing with a fixed bed reactor, where the bacteria are fixed on supports. Thus, formally there is no dilution term in the balance equations. However, on the other hand, it was noted that a portion of the biomass was detached: it was hypothesized that the rate of detachment was proportional to the rate of dilution, represented by coefficient α. Under these conditions, the model is rewritten as follows:

$$\frac{dX_1}{dt} = \mu_1 X_1 - \alpha D X_1 \tag{3.43}$$

$$\frac{dX_2}{dt} = \mu_2 X_2 - \alpha D X_2 \tag{3.44}$$

$$\frac{dS_1}{dt} = D(S_{1\text{in}} - S_1) - k_1 \mu_1 X_1 \tag{3.45}$$

$$\frac{dS_2}{dt} = D(S_{2\text{in}} - S_2) + k_2 \mu_1 X_1 - k_3 \mu_2 X_2 \tag{3.46}$$

$$\frac{dZ}{dt} = D(Z_{\text{in}} - Z) \tag{3.47}$$

$$\frac{dC}{dt} = D(C_{\text{in}} - C) - q_C + k_4 \mu_1 X_1 + k_5 \mu_2 X_2 \tag{3.48}$$

$$q_C = k_L a(C - S_2 - Z - K_H P_C) \tag{3.49}$$

$$P_C = \frac{\phi - \sqrt{\phi^2 - 4K_H P_T(C + S_2 - Z)}}{2K_H} \tag{3.50}$$

$$\phi = C + S_2 - Z + K_H P_T + \frac{k_6}{k_L a}\mu_2 X_2 \tag{3.51}$$

$$q_M = k_6 \mu_2 X_2 \tag{3.52}$$

$$pH = -log_{10}\left(K_b \frac{C - Z + S_2}{Z - S_2}\right) \tag{3.53}$$

In addition, growth models were chosen, one Monod model for acidogenesis and one Haldane model for methanization:

$$\mu_1 = \frac{\mu_{\max 1} S_1}{K_{S1} + S_1}, \qquad \mu_2 = \frac{\mu_0 S_2}{K_{S2} + S_2 + S_2^2/K_{I2}} \tag{3.54}$$

In the absence of systematic rule, this choice was dictated by a desire to have kinetic models that are sufficiently simple, coherent with those normally used for anaerobic digestion, but also capable of highlighting the potential instability of the process in the presence of the accumulation of volatile fatty acids (explaining the choice of the Haldane model for μ_2).

Knowing that K_b and K_H are known chemical and physical constants (K_b = 6.5 10^{-7} mol/l, K_H = 16 mmol/l/atm), we note that the model contains 13 parameters to be identified. In addition, the variables available for the measurement are the dilution rate D, the inlet concentrations, $S_{1\text{in}}$, $S_{2\text{in}}$, Z_{in}, C_{in}, the gas flow rates q_C, q_M, the concentrations S_1, S_2, Z, C, and the pH.

3.6.2. *Experiment design*

Given the complexity of the model and the large number of parameters as well as the experimental constraints (long time constants and potential instability of the process), the strategy followed here for experiment design consisted of covering a number of operating points sufficiently representative of how the process works. The experiment design is given in Table 3.1.

3.6.3. *Choice of data for calibration and validation*

In this case, one of the priorities was to obtain a model, which would be capable of correctly reproducing as a priority the equilibrium conditions. This is why the data collected were separated into two categories: the data corresponding to the steady-state conditions for calibrating the parameters and the dynamic data for the validation. The periods corresponding to the values used for the calibration are represented in Figures 3.5 and 3.6 by a bold line on the abscissa.

$\mathbf{D(day^{-1})}$	S_{1in} **(g/l)**	S_{2in} **(mmole/l)**	**pH**
0.34	9.5	93.6	5.12
0.35	10	73.68	4.46
0.35	4.8	38.06	4.49
0.36	15.6	112.7	4.42
0.26	10.6	72.98	4.42
0.51	10.7	71.6	4.47
0.53	9.1	68.78	5.30

Table 3.1. *Characteristics of average feed conditions*

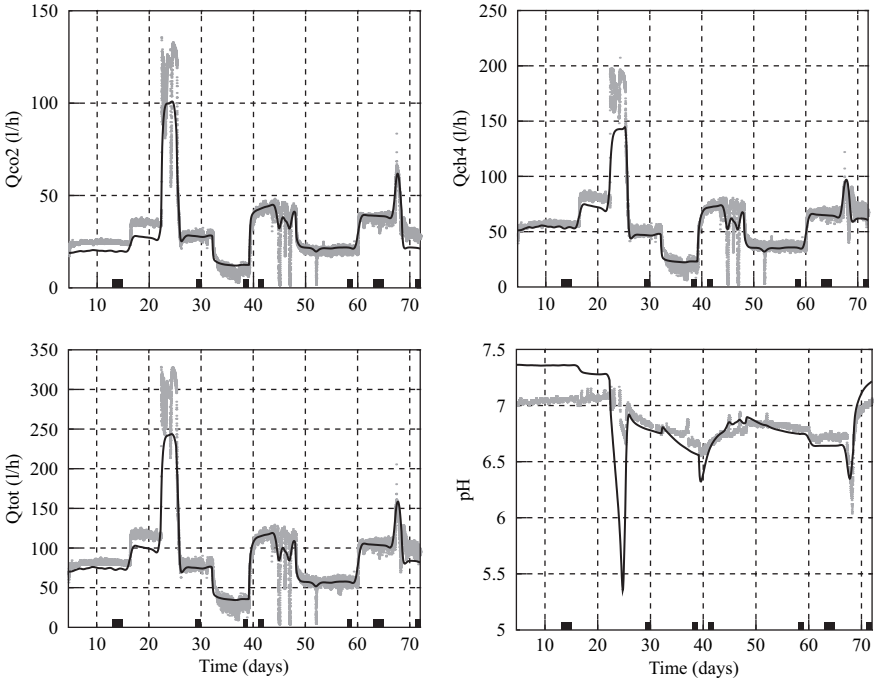

Figure 3.5. *Simulated values (fine line) and data values (thick line) of gas flow and pH. The periods used for the calibration are represented in bold on the abscissa*

3.6.4. *Parameter identification*

With such a complex model, we can expect to encounter problems of structural and practical identifiability. We expect to be in a position to alleviate, at least partially,

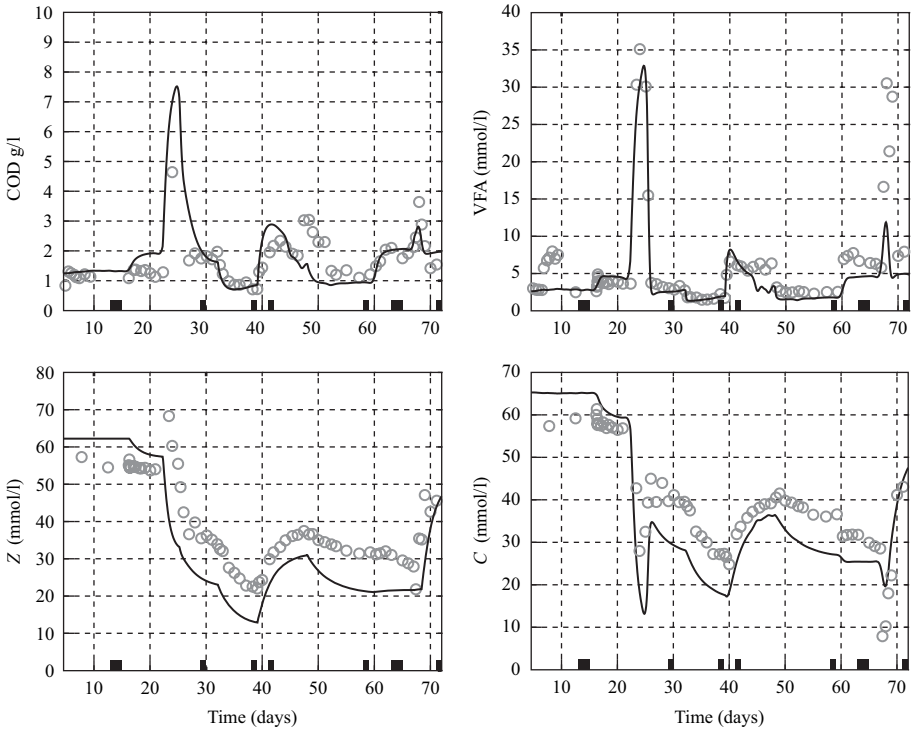

Figure 3.6. *Simulated values (continuous line) and data values (o) of S_1, S_2, Z and C. The periods used for the calibration are represented in bold on the abscissa*

the problems of practical identifiability, thanks to experiment design. However, what about the problems of structural identifiability? Without prejudging the results of an analysis, which could turn out to be complex, it seems to be interesting to take advantage of the structure of the model and its properties for formulating the problem of identification of parameters in a different form. We will see in the next chapter (state observers) that there is a state transformation (4.42)[2] which enables us to rewrite a portion of the model in a form independent of the kinetics. This transformation is doubly interesting in our case. On the one hand, it enables us to proceed with the identification of kinetic and other model parameters in a distinct manner. On the other hand, this separation is of particular interest insofar as the kinetic modeling is its weakest link, given that we lack the physical base for the choice of an appropriate model and in addition, it is the chief source of nonlinearities in the model.

2. This transformation is presented in detail and in a more general form in [BAS 90].

It is basically this approach that was adopted here. As the identification is carried out on the basis of the steady-state data, static balance equations of biomasses X_1 and X_2 and the expressions for the specific growth rates, we derive the following expressions:

$$\frac{1}{D} = \frac{\alpha}{\mu_{1\,\max}} + K_{S1}\frac{\alpha}{\mu_{1\,\max}}\frac{1}{\bar{S}_1} \tag{3.55}$$

$$\frac{1}{D} = \frac{\alpha}{\mu_0} + K_{S2}\frac{\alpha}{\mu_0}\frac{1}{\bar{S}_2} + \frac{1}{K_{I2}}\frac{\alpha}{\mu_0}\bar{S}_2 \tag{3.56}$$

These equations are linear in the parameters $\frac{\alpha}{\mu_{1\,\max}}$, $K_{S1}\frac{\alpha}{\mu_{1\,\max}}$, $\frac{\alpha}{\mu_0}$, $K_{S2}\frac{\alpha}{\mu_0}$ and $\frac{1}{K_{I2}}\frac{\alpha}{\mu_0}$. They can be determined through linear regression. The only problem is that it is not possible to distinguish between $\mu_{1\,\max}$ and α; this is why we have considered a value from the literature ([GHO 74]) for $\mu_{1\,\max}$. This choice turns out to be even more acceptable, and a sensitivity analysis shows a low sensitivity of $\mu_{1\,\max}$.

We can thus use the equation for the CO_2 flow rate for determining k_La, by recalling that $q_C = k_La(CO_2 - K_HP_C)$ and that the reaction for the dissociation of bicarbonate enables the linking of CO_2 to C and to pH according to the relationship:

$$CO_2 = C\frac{1}{1 + K_b10^{pH}} \tag{3.57}$$

This enables us to determine the kinetic parameters and the transfer parameters independently of the performance coefficients. The results are summarized in Table 3.2.

Parameter	Units	Value	Standard deviation
$\mu_{1\,\max}$	$textDay^{-1}$	1.2	(1)
K_{S1}	g/l	7.1	5.0
μ_0	$textDay^{-1}$	0.74	0.9
K_{S2}	mmol	9.28	13.7
K_{I2}	mmol	16	17.9
α	/	0.5	0.4
k_La	Day^{-1}	19.8	3.5

Table 3.2. *Estimated values of kinetic and transfer parameters. (1) taken from [GHO 74]*

The values of the yield coefficients now have to be calculated. The main difficulty results from the absence of measurements of populations X_1 and X_2. Without these measurements, it turns out that the yield coefficients are not structurally identifiable. This can be shown by considering, for example, a rescaling for X_1 and X_2: $X_1' = \lambda_1 X_1$, $X_2' = \lambda_2 X_2$. This rescaling can be compensated by putting the yield coefficients in scale as follows

$$k_1' = \frac{k_1}{\lambda_1},\ k_2' = \frac{k_2}{\lambda_1},\ k_4' = \frac{k_4}{\lambda_1},\ k_3' = \frac{k_3}{\lambda_2},\ k_5' = \frac{k_5}{\lambda_2},\ k_6' = \frac{k_6}{\lambda_2} \tag{3.58}$$

In order to overcome the difficulty, the identification is carried out in two stages: first, the estimation of the structurally identifiable ratios of the yield coefficients (k_2/k_1, k_6/k_3, k_5/k_3, k_4/k_1); second, the use of the data of volatile suspended solids (VSS) in order to determine the values of each performance coefficient. The estimation of the ratios of performance coefficients is performed on the basis of balance equations in steady state, which can be rewritten as follows after eliminating X_1 and X_2:

$$q_C = D(C_{\text{in}} - C) + \left(\frac{k_4}{k_1} + \frac{k_2 k_5}{k_1 k_3}\right) D(S_{1\text{in}} - S_1) + \frac{k_5}{k_3} D(S_{2\text{in}} - S_2)$$

$$q_M = \frac{k_2 k_6}{k_1 k_3} D(S_{1\text{in}} - S_1) + \frac{k_6}{k_3} D(S_{2\text{in}} - S_2)$$

The ratios $\frac{k_4}{k_1} + \frac{k_2 k_5}{k_1 k_3}$, $\frac{k_5}{k_3}$, $\frac{k_2 k_6}{k_1 k_3}$, $\frac{k_6}{k_3}$ can thus be determined using linear regression. The result of the calibration is presented in Table 3.3.

Ratio	Units	Value	Standard deviation
k_2/k_1	mmol/g	2.72	2.16
k_6/k_3	/	1.62	0.12
k_5/k_3	/	1.28	0.13
k_4/k_1	mmol/g	1.18	3.02

Table 3.3. *Estimated values of the ratios of performance coefficients*

The determination of the coefficients is thus made on the basis of VSS measurements. In fact, the VSS represents an approximate indicator of $X_1 + X_2$. The determination of the VSS distribution between the two bacterial populations has been performed by considering a ratio ($= 0.2$) between the acidogenic bacteria X_1 and the total biomass $X_1 + X_2$ taken from [SAN 94]. The results are presented in Table 3.4.

Parameter	Units	Value	Standard deviation
k_1	g S_1 /g X_1	42.14	18.94
k_2	mmol S_2 /g X_1	116.5	113.6
k_3	mmol S_2 /g X_2	268	52.31
k_4	mmol CO_2 /g X_1	50.6	143.6
k_5	mmol CO_2 /g X_2	343.6	75.8
k_6	mmol CH_4 /g X_2	453.0	90.9

Table 3.4. *Estimated values of performance coefficients*

3.6.5. *Analysis of the results*

The first essential stage after the calibration of parameters is their validation for the set of data not used for the calibration. This can be seen in Figures 3.5 and 3.6. We can generally see a good fit between the model and the transient experimental data. This demonstrates the interest in a systematic approach for the identification of parameters, all the more in a case as difficult and complex as this one.

However, the reliability of the estimated values of the parameters remains to be evaluated. This corresponds to the standard deviation of each parameter shown in Tables 3.2, 3.3 and 3.4. The increase in this value should be noted while converting the ratios of the performance coefficient to their individual values. This reflects the large uncertainty associated with the determination of biomass concentrations on the basis of VSS data and the assumed ratio of their distribution. We will also note the rather high uncertainty of kinetic parameters, which is not at all surprising, given the fact that the chosen structures are heuristic. Finally, in the ratios of performance coefficients, a worse reliability is found for the parameters involving k_1, which is probably an effect of the variable nature of the concentration of feed $S_{1\text{in}}$.

3.7. Bibliography

[ABO 78] S. ABORHEY and D. WILLIAMSON, "State and parameter estimation of microbial growth processes", *Automatica*, vol. 14, pp. 493–498, 1978.

[BAL 94] M. BALTES, R. SCHNEIDER, C. STURM and M. REUSS, "Optimal experimental design for parameter estimation in unstructured growth models", *Biotechnol. Prog.*, vol. 10, pp. 480–488, 1994.

[BAS 90] G. BASTIN and D. DOCHAIN, *On-line Estimation and Adaptive Control of Bioreactors*, Elsevier, Amsterdam, 1990.

Chapter 7

Adaptive Linearizing Control and Extremum-Seeking Control of Bioprocesses

7.1. Introduction

Industrial-scale biotechnological processes have progressed vigorously over recent decades. As already mentioned, the problems arising from the implementation of these processes are similar to those of more classical industrial processes and the need for automatic control in order to optimize production efficiency, improve product quality or detect disturbances in process operation is obvious. Nevertheless, automatic control of industrial biotechnological processes is facing two major difficulties:

a) it remains difficult to develop models taking into account the numerous factors that can influence microorganism growth and other biochemical reactions;

b) another essential difficulty lies in the absence, in most cases, of cheap and reliable instrumentation suited to real-time monitoring.

The classical monitoring and control methods do not prove very efficient to tide over these difficulties. The efficiency of any control system highly depends on the design of the control and monitoring techniques and the care taken in their design. In fact, monitoring or control algorithms will prove to be efficient if they are able to incorporate the important well-known information on the process while being able to deal with the missing information (lack of online measurements, uncertainty on the dynamics, etc.) in a "robust" way, i.e. such that the missing information will not significantly

---

Chapter written by Denis DOCHAIN, Martin GUAY, Michel PERRIER and Mariana TITICA.

deteriorate the control performance of the process. The versatility of computing platforms greatly facilitates the design and implementation of sophisticated controllers (beyond the classical PID as presented in Chapter 6). These controllers may arise from quite complex theory (nonlinear control, adaptive control, extremum-seeking control) but, as will be shown, their structure and implementation will remain rather simple while including the key features of simple PIDs.

In this chapter, we shall show how to incorporate the well-known features of the dynamics of biochemical processes (basically, the reaction network and the material balances) in control algorithms which are capable of dealing with process uncertainty (in particular on the reaction kinetics) by introducing, an adaptation scheme for example in the control algorithms.

It is also important to draw to the attention of the reader that these control systems are not just the object of academic research but are already used in several applications (see e.g. [BAS 90, CHE 91]). Adaptive as well as non-adaptive linearizing control of bioreactors has been a quite active research area over recent decades. In addition to the works by the authors of this chapter and their colleagues, let us also mention e.g. [ALV 88, CHI 91, DAH 91, FLA 91, GOL 86, HEN 92, HOO 86].

The chapter is organized as follows. We shall first concentrate on the design of adaptive linearizing controllers for bioprocesses based on a reduced order model of the process. The methodology will be illustrated by anaerobic digestion and activated sludge. We shall then consider online optimization approaches, adaptive extremum-seeking control, whose specificity is to combine feedback control with a search algorithm for the optimal process operating conditions. In that section, we shall consider the illustrative example of fed-batch reactors.

7.2. Adaptive linearizing control of bioprocesses

7.2.1. *Design of the adaptive linearizing controller*

Let us first concentrate on the design of model-based controllers for bioreactors. The key idea of the control design is here again to take advantage of what is well known about the dynamics of bioprocesses (reaction network and mass balances) which are summarized in the general dynamic model already presented in the preceding chapters:

$$\frac{d\xi}{dt} = Kr(\xi) + F - Q - D\xi \tag{7.1}$$

while taking into account the model uncertainty (mainly the kinetics). Since the model is generally nonlinear, the model-based control design will result in a *linearizing* control structure, in which the online estimation of the unknown variables (component

The auxiliary variables ζ, the unknown parameters and tuning estimation variables have been initialized as follows:

$$\zeta_1 = 1400\,\text{mg/l},\ \zeta_2 = 750\,\text{mg/l},\ \zeta_3 = 1400\,\text{mg/l},\ g_{1,0} = g_{2,0} = 10^{-3}$$
$$\gamma_1 = \gamma_2 = 0.9,\ \hat{\alpha}_{1,0} = \hat{\alpha}_{2,0} = 0.00025\,\text{l}^2/\text{mg}^2/\text{h}$$

Note the ability of the controller to maintain the controlled outputs S and C close to their desired values in spite of the unknown disturbance.

7.3. Adaptive extremum-seeking control of bioprocesses

Most adaptive control schemes documented in the literature (e.g. [AST 95, GOO 84, KRS 95, NAR 89]) are developed for regulation to known set-points or tracking known reference trajectories. In some applications, however, the control objective could be to optimize an objective function which can be a function of unknown parameters, or to select the desired values of the state variables to keep a performance function at its extremum value. Self-optimizing control and extremum-seeking control are two methods of handling these types of optimization problems. The task of extremum seeking is to find the operating set-points that maximize or minimize an objective function. Since the early research work on extremum control in the 1920s [LEB 22], several applications of extremum control approaches have been reported (e.g. [AST 95, DRK 95, STE 80, VAS 57]). Krstic *et al.* [KRS 00a, KRS 00b] presented several extremum control schemes and stability analysis for extremum-seeking of linear unknown systems and a class of general nonlinear systems [KRS 00a, KRS 00b, KRS 98]. A neural network-based approach has been proposed in [LI 95].

The implications for the biochemical industry are clear. In this sector, it is recognized that even small performance improvements in key process control variables may result in substantial economic gains. As an example, the potential benefits of extremum-seeking techniques in the maximization of biomass production rate in well-mixed biological processes has been demonstrated in [WAN 99].

The proposed scheme utilizes explicit structure information of the objective function that depends on system states and unknown plant parameters. This scheme is based on Lyapunov's stability theorem. As a result, global stability is ensured during the seeking of the extremum of the nonlinear stirred tank bioreactors. It is also shown that once a certain level of persistence of excitation (PE) condition is satisfied, the convergence of the extremum-seeking mechanism can be guaranteed. In this section we concentrate on the adaptive extremum-seeking control of bioreactors operating in the fed-batch mode (see also [TIT 03a, TIT 03b]) but several other alternatives of the similar schemes (including the use of universal approximation like artificial neural networks (ANN)) have been proposed in the literature for different bioprocess configurations [GUA 04, HAR 06, MAR 04, MAR 03, ZHA 02].

7.3.1. *Fed-batch reactor model*

Fed-batch bioreactors represent an important class of bioprocesses, mainly in the food industry and in the pharmaceutical industry but also e.g. for biopolymer applications (PHB). One of the key issues in the operation of fed-batch reactors is to optimize the production of a synthesis product (e.g. penicillin, enzymes, etc.) or biomass (e.g. baker's yeast). They are therefore ideal candidates for optimal control strategies. A intensive research activity was devoted to optimal control of (fed-batch) bioreactors mainly in the 1970s and in the 1980s (see e.g. [OHN 76, CHE 79, PAR 85, PER 79]). However, in practice, because of the large uncertainty related to the modeling of the process dynamics [BAS 90], poor performance may be expected from such control strategies, and although a priori attractive, optimal control has not been largely applied to industrial bioprocesses. Alternative approaches have been proposed for handling the process uncertainties with an adaptive control scheme (e.g. [DOC 89, VAN 93]). In this approach, we propose to go a step further by including a static optimum search in the adaptive control scheme.

Consider the following dynamic model of a simple microbial growth process with one gaseous product in a fed-batch reactor:

$$\frac{dX}{dt} = \mu X - DX \tag{7.52}$$

$$\frac{dS}{dt} = -k_1 \mu X + D(S_0 - S) \tag{7.53}$$

$$y = k_2 \mu X \tag{7.54}$$

$$\frac{dv}{dt} = Dv \tag{7.55}$$

where states X (g/l) and S (g/l) hold for biomass and substrate concentrations, respectively. μ (h^{-1}) is the specific growth rate, D (h^{-1}) is the dilution rate, y (g/l/h) is the production rate of the reaction product, S_0 (g/l) denotes the concentration of the substrate in the feed, k_1, k_2 are yield coefficients, and v (l) is the volume of liquid medium in the tank. A typical situation in bioprocess applications is when the biomass concentration is not available for online measurement while the gaseous outflow rate y (e.g. CO_2) is easier to measure online. We consider here that only S and y are measurable while the biomass concentration X is not available for feedback control.

In this work, we consider the extremum-seeking problem for the bioprocess model (7.52)-(7.55) with a specific growth rate μ expressed by the Haldane model. This model (see Figure 7.3) is given by:

$$\mu = \frac{\mu_0 S}{K_S + S + \frac{S^2}{K_I}} \tag{7.56}$$

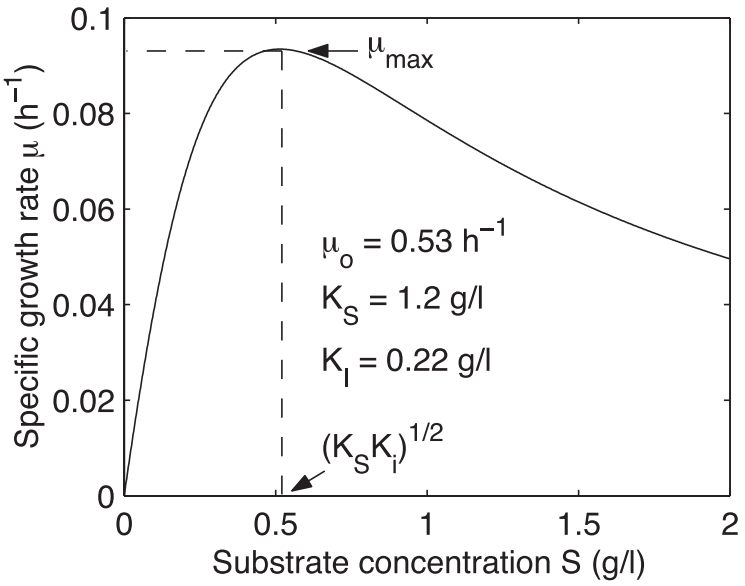

Figure 7.3. *Haldane model*

where μ_0 is a parameter related to the maximum value of the specific growth rate as follows: $\mu_0 = \mu_{\max}(1 + 2\sqrt{\frac{K_S}{K_I}})$. Coefficients K_S and K_I denote the saturation constant and the inhibition constant, respectively. The Haldane model is a growth model commonly used in situations where substrate inhibition is important. This situation is typical of fed-batch bioreactors. The control objective is to design a controller with D as the control action such that the biomass production VX achieves its maximum at the end of the fed-batch operation. It is well-known (e.g. [BAS 90]) that the maximization will be completed if the specific growth rate is kept at its maximum value:

$$S^* = \sqrt{K_S K_I} \tag{7.57}$$

From the above considerations, we know that if the substrate concentration S can be stabilized at the set-point S^* then the production of biomass is maximized. However, since the exact values of the Haldane model parameters K_S, μ_0 and K_I are usually unknown, the desired set-point S^* is not available. In this work, an adaptive extremum-seeking algorithm is developed to search this unknown set-point such that the biomass production at the end of the reactor operation, i.e. $v(t_f)X(t_f)$ (with t_f the final time of the fed-batch operation) is maximized.

In the technical developments here below, we shall consider the following assumption for parameters K_S and K_I of the Haldane model.

Assumption: K_S and K_I are known to be bounded as follows: $K_{S,\min} \leq K_S \leq K_{S,\max}$, $0 < K_I \leq K_{I,\max}$.

This assumption is only important for the technical developments in order to avoid singularities in the extremum-seeking controller. It should not be interpreted as a "microbial" constraint on the kinetic model.

7.3.2. *Estimation and controller design*

The design of the adaptive extremum-seeking controller will proceed in different steps. First of all, we shall start with the estimation equation for y, then include the controller equations and the estimation equations for the unknown parameters in a Lyapunov-based derivation framework, and end up with the stability and convergence analysis arguments.

7.3.2.1. *Estimation equation for the gaseous outflow rate y*

Let us start with the parameter estimation algorithm for the unknown parameters K_S, K_I and μ_0. The ratio of the yield coefficients $\frac{k_1}{k_2}$ is assumed to be known. It follows from (7.54) that:

$$\mu X = \frac{y}{k_2} \tag{7.58}$$

Then equations (7.52)-(7.53) can be reformulated as follows:

$$\frac{dX}{dt} = \frac{1}{k_2} y - DX \tag{7.59}$$

$$\frac{dS}{dt} = -\frac{k_1}{k_2} y + D(S_0 - S) \tag{7.60}$$

By considering equations (7.54)-(7.56) and (7.59)-(7.60), the time derivative of y is equal to:

$$\begin{aligned} \frac{dy}{dt} = {} & k_2 \mu_0 X \frac{K_S - S^2/K_I}{\left(K_S + S + S^2/K_I\right)^2} \left(- \frac{k_1}{k_2} y + D(S_0 - S) \right) \\ & + k_2 \mu \left[\frac{1}{k_2} y - DX \right] \end{aligned} \tag{7.61}$$

Since the biomass concentration X is not accessible for online measurement, we reformulate $\frac{dy}{dt}$ by replacing X with $\frac{y}{k_2 \mu}$ as follows:

$$\frac{dy}{dt} = \frac{K_s - \frac{S^2}{K_I}}{S\left(K_S + S + \frac{S^2}{K_I}\right)} \left(- \frac{k_1}{k_2} y^2 + D\big(S_0 - S\big) y \right) + \mu y - Dy \tag{7.62}$$

Let $\theta = [\theta_s \quad \theta_\mu \quad \theta_i]^T$ with $\theta_\mu = \frac{\mu_0}{K_S}, \theta_s = \frac{1}{K_S}, \theta_i = \frac{1}{K_I K_S}$, and define $\theta_k = \frac{k_1}{k_2}$. Equations (7.60) and (7.62) can then be rewritten as follows:

$$\frac{dS}{dt} = -\theta_k y + D\big(S_0 - S\big) \tag{7.63}$$

$$\begin{aligned}\frac{dy}{dt} &= \frac{1 - \theta_i S^2}{S\big(1 + \theta_s S + \theta_i S^2\big)}\big(D\big(S_0 - S\big) - \theta_k y\big)y \\ &\quad + \frac{\theta_\mu S y}{1 + \theta_s S + \theta_i S^2} - uy\end{aligned} \tag{7.64}$$

Let $\hat{\theta}$ denote the estimate of the true parameter θ, and $\hat{y}$ be the prediction of y by using the estimated parameter $\hat{\theta}$. The predicted state $\hat{y}$ is generated by the following equation:

$$\begin{aligned}\frac{d\hat{y}}{dt} &= \frac{1 - \hat{\theta}_i S^2}{S\big(1 + \hat{\theta}_s S + \hat{\theta}_i S^2\big)}\big(D\big(S_0 - S\big) - \theta_k y\big)y \\ &\quad + \frac{\hat{\theta}_\mu S y}{1 + \hat{\theta}_s S + \hat{\theta}_i S^2} - Dy + k_y e_y\end{aligned} \tag{7.65}$$

with $k_y > 0$ and the prediction error $e_y = y - \hat{y}$. It follows from (7.63)-(7.65) that:

$$\begin{aligned}\frac{de_y}{dt} &= -k_y e_y + \frac{1 - \theta_i S^2}{s\big(1 + \theta_s S + \theta_i S^2\big)}\big(D\big(S_0 - S\big) - \theta_k y\big)y \\ &\quad + \frac{\theta_\mu S y}{1 + \theta_s S + \theta_i S^2} - \frac{1 - \hat{\theta}_i S^2}{S\big(1 + \hat{\theta}_s S + \hat{\theta}_i S^2\big)}\big(D\big(S_0 - S\big) - \theta_k y\big)y \\ &\quad - \frac{\hat{\theta}_\mu S y}{1 + \hat{\theta}_s S + \hat{\theta}_i S^2}\end{aligned} \tag{7.66}$$

7.3.2.2. *Design of the adaptive extremum-seeking controller*

The desired set-point (7.57) can be re-expressed as follows:

$$S^* = \frac{1}{\sqrt{\theta_i}} \tag{7.67}$$

Since parameter θ_i is unknown, we design a controller to drive the substrate concentration S to:

$$\frac{1}{\sqrt{\hat{\theta}_i}}$$

i.e. an estimate of the unknown optimum S^*. An excitation signal is then designed and injected into the adaptive system such that the estimated parameter $\hat{\theta}_i$ converges to its true value. The extremum-seeking control objective can be achieved when the substrate concentration S is stabilized at the optimal operating point S^*.

Define the "control" error z_s:

$$z_s = S - \frac{1}{\sqrt{\hat{\theta}_i}} - d(t) \tag{7.68}$$

where $d(t) \in C^1$ is a dither signal that will be assigned later. The time derivative of z_s is given by:

$$\frac{dz_s}{dt} = D\big(S_0 - S\big) - \theta_k y + \frac{1}{2}\hat{\theta}_i^{-\frac{3}{2}}\frac{d\hat{\theta}_i}{dt} - \dot{d}(t) = \Gamma_1 \tag{7.69}$$

We consider a Lyapunov function candidate:

$$V = \frac{z_s^2}{2} + \frac{1}{2}\left(\frac{\tilde{\theta}_\mu^2}{\gamma_\mu} + \frac{\tilde{\theta}_s^2}{\gamma_s} + \frac{\tilde{\theta}_i^2}{\gamma_i}\right) + \big(1 + \theta_s S + \theta_i S^2\big)\frac{e_y^2}{2} \tag{7.70}$$

with constants $\gamma_\mu, \gamma_s, \gamma_i > 0$. Taking the time derivative of V and substituting (7.63), (7.69) and (7.66) leads to:

$$\begin{aligned}
\frac{dV}{dt} &= z_s\Gamma_1 - \frac{\tilde{\theta}_\mu}{\gamma_\mu}\frac{d\hat{\theta}_\mu}{dt} - \frac{\tilde{\theta}_s}{\gamma_s}\frac{d\hat{\theta}_s}{dt} - \frac{\tilde{\theta}_i}{\gamma_i}\frac{d\hat{\theta}_i}{dt} \\
&\quad + e_y\frac{\big(1 - \theta_i S^2\big)}{S}\big(D\big(S_0 - S\big) - \theta_k y\big)y + e_y\theta_\mu S y \\
&\quad - e_y\left(\frac{1 - \hat{\theta}_i S^2}{S\big(1 + \hat{\theta}_s S + \hat{\theta}_i S^2\big)}\big(D\big(S_0 - S\big) - \theta_k y\big)y\right. \\
&\qquad \left. + \frac{\hat{\theta}_\mu S y}{1 + \hat{\theta}_s S + \hat{\theta}_i S^2}\right)\big(1 + \theta_s S + \theta_i S^2\big) \\
&\quad - e_y^2\left[\left(k_y - \frac{\big(\theta_s + 2\theta_i S\big)\big(S_0 - S\big)D}{2\big(1 + \theta_s S + \theta_i S^2\big)}\right)\big(1 + \theta_s S + \theta_i S^2\big)\right. \\
&\qquad \left. + \frac{1}{2}\big(\theta_s + 2\theta_i S\big)\theta_k y\right]
\end{aligned} \tag{7.71}$$

Defining the functions:

$$\begin{aligned}
\tilde{\Gamma} &= -e_y^2\left(k_y - \frac{\big(\theta_s + 2\theta_i S\big)\big(S_0 - S\big)D}{2\big(1 + \theta_s S + \theta_i S^2\big)}\right)\big(1 + \theta_s S + \theta_i S^2\big) \\
&\quad - \frac{1}{2}e_y^2\big(\theta_s + 2\theta_i S\big)\theta_k y
\end{aligned} \tag{7.72}$$

$$\Psi_i = \Gamma_3 D + \Gamma_4 \tag{7.73}$$

$$\Psi_\mu = e_y S y \tag{7.74}$$

$$\Psi_s = \Gamma_5 D + \Gamma_6 \tag{7.75}$$

where:

$$\Gamma_3 = -e_y S\big(S_0 - S\big)y - \frac{e_y S\big(1-\hat{\theta}_i S^2\big)\big(S_0 - S\big)y}{1+\hat{\theta}_s S + \hat{\theta}_i S^2} \tag{7.76}$$

$$\Gamma_4 = e_y S\theta_k y^2 + \frac{e_y S\big(1-\hat{\theta}_i S^2\big)\theta_k y^2}{1+\hat{\theta}_s S + \hat{\theta}_i S^2} - \frac{e_y S^3 \hat{\theta}_\mu y}{1+\hat{\theta}_s S + \hat{\theta}_i S^2} \tag{7.77}$$

$$\Gamma_5 = -\frac{e_y\big(1-\hat{\theta}_i S^2\big)\big(S_0 - S\big)y}{1+\hat{\theta}_s S + \hat{\theta}_i S^2} \tag{7.78}$$

$$\Gamma_6 = \frac{e_y\big(1-\hat{\theta}_i S^2\big)\theta_k y^2}{1+\hat{\theta}_s S + \hat{\theta}_i S^2} - \frac{e_y \hat{\theta}_\mu S^2 y}{1+\hat{\theta}_s S + \hat{\theta}_i S^2} \tag{7.79}$$

we can write $\frac{dV}{dt}$ as follows:

$$\begin{aligned}\frac{dV}{dt} = z_s\bigg[D\big(S_0 - S\big) - \theta_k y + \frac{1}{2}\hat{\theta}_i^{-\frac{3}{2}}\frac{d\hat{\theta}_i}{dt} - \dot{d}(t)\bigg] + \bigg(\Psi_i - \frac{1}{\gamma_i}\frac{d\hat{\theta}_i}{dt}\bigg)\tilde{\theta}_i \\ + \bigg(\Psi_\mu - \frac{1}{\gamma_\mu}\frac{d\hat{\theta}_\mu}{dt}\bigg)\tilde{\theta}_\mu + \bigg(\Psi_s - \frac{1}{\gamma_s}\frac{d\hat{\theta}_s}{dt}\bigg)\tilde{\theta}_s + \tilde{\Gamma}\end{aligned} \tag{7.80}$$

For the solution of the extremum-seeking problem, we pose the dynamic state feedback:

$$\dot{d}(t) = a(t) + \frac{1}{2}\hat{\theta}_i^{-\frac{3}{2}}\frac{d\hat{\theta}_i}{dt} - k_d d(t) \tag{7.81}$$

$$D = \frac{1}{S_0 - S}\big[-k_z z_s + \theta_k y + a(t) - k_d d(t)\big], \quad k_z > 0 \tag{7.82}$$

where $a(t)$ acts as a dither signal on the closed-loop process and k_d is a strictly positive constant.

The substitution of (7.82) in (7.80) yields:

$$\frac{dV}{dt} = -k_z z_s^2 + \bigg(\Psi_i - \frac{\dot{\hat{\theta}}_i}{\gamma_i}\bigg)\tilde{\theta}_i + \bigg(\Psi_\mu - \frac{\dot{\hat{\theta}}_\mu}{\gamma_\mu}\bigg)\tilde{\theta}_\mu + \bigg(\Psi_s - \frac{\dot{\hat{\theta}}_s}{\gamma_s}\bigg)\tilde{\theta}_s\tilde{\Gamma} + \tilde{\Gamma} \tag{7.83}$$

Using the definition of Ψ_i and Ψ_s, we express (7.83) as:

$$\begin{aligned}\frac{dV}{dt} = -k_z z_s^2 + \bigg(\Gamma_3 D + \Gamma_4 - \frac{\dot{\hat{\theta}}_i}{\gamma_i}\bigg)\tilde{\theta}_i + \bigg(\Psi_\mu - \frac{\dot{\hat{\theta}}_\mu}{\gamma_\mu}\bigg)\tilde{\theta}_\mu \\ + \bigg(\Gamma_5 D + \Gamma_6 - \frac{\dot{\hat{\theta}}_s}{\gamma_s}\bigg)\tilde{\theta}_s\tilde{\Gamma}\end{aligned} \tag{7.84}$$

We propose the following update law as follows:

$$\dot{\hat{\theta}}_i = \begin{cases} \gamma_i\big(\Gamma_3 D + \Gamma_4\big), & \text{if } \hat{\theta}_i > \epsilon_i \text{ or } \hat{\theta}_i = \epsilon_i \text{ and } \big(\Gamma_3 D + \Gamma_4\big) > 0 \\ 0 & \text{otherwise} \end{cases} \tag{7.85}$$

$$\dot{\hat{\theta}}_s = \begin{cases} \gamma_s\big(\Gamma_5 D + \Gamma_6\big), & \text{if } \hat{\theta}_s > \epsilon_s \text{ or } \hat{\theta}_s = \epsilon_s \text{ and } \big(\Gamma_5 D + \Gamma_6\big) > 0 \\ 0 & \text{otherwise} \end{cases} \tag{7.86}$$

$$\dot{\hat{\theta}}_\mu = \gamma_\mu \Psi_\mu \tag{7.87}$$

with the initial condition $\hat{\theta}_s(0) \geq \epsilon_s = \frac{1}{K_{S,\max}} > 0$, and $\hat{\theta}_i(0) \geq \epsilon_i = \frac{1}{K_{s,\max} K_{I,\max}} > 0$. The update laws (7.85)-(7.86) are projection algorithms that ensure that $\hat{\theta}_s(t) \geq \epsilon_s > 0$ and $\hat{\theta}_i(t) \geq \epsilon_i > 0$. They also ensure that:

$$\left(\Gamma_3 D + \Gamma_4 - \frac{\dot{\hat{\theta}}_i}{\gamma_i}\right)\tilde{\theta}_i + \left(\Psi_\mu - \frac{\dot{\hat{\theta}}_\mu}{\gamma_\mu}\right)\tilde{\theta}_\mu + \left(\Gamma_5 D + \Gamma_6 - \frac{\dot{\hat{\theta}}_s}{\gamma_s}\right)\tilde{\theta}_s \leq 0, \tag{7.88}$$

7.3.2.3. *Stability and convergence analysis*

Substituting the update laws (7.85)-(7.86) into (7.84), we obtain:

$$\frac{dV}{dt} \leq -k_z z_s^2 + \tilde{\Gamma} \tag{7.89}$$

We then assign the gain function k_y such that the term $\tilde{\Gamma}$ is negative. Using (7.72), we consider:

$$k_y = k_{y0} + \frac{\big(S_0 - S\big)|D|}{\epsilon(S + \epsilon)} \tag{7.90}$$

with positive constants $k_{y0} > 0$ and $0 < \epsilon \ll 1$. As a result, we obtain:

$$\frac{dV}{dt} \leq -k_z z_s^2 - k_{y0}\big(1 + \theta_s S + \theta_i S^2\big)e_y^2 \tag{7.91}$$

as required. Following LaSalle-Yoshizawa's Theorem, it is concluded that $\hat{\theta}$, z_s and e_y are bounded, and:

$$\lim_{t\to\infty} z_s = 0, \qquad \lim_{t\to\infty} e_y = 0 \tag{7.92}$$

This implies that:

$$\lim_{t\to\infty} \dot{\hat{\theta}}_i(t) = 0, \qquad \lim_{t\to\infty} \dot{\hat{\theta}}_\mu(t) = 0, \qquad \lim_{t\to\infty} \dot{\hat{\theta}}_s(t) = 0.$$

Hence, the auxiliary variable $d(t)$ is bounded if $a(t)$ is bounded and $d(t)$ tends towards zero if $a(t)$ does. Thus, all signals of the closed-loop system are bounded. It should be noted that the convergence of the state error e_y does not mean that the estimated parameters converge to their true values as $t \rightarrow \infty$. In section 7.4, we investigate the condition that guarantees the parameter convergence.

7.3.2.4. *A note on dither signal design*

The results of the previous section confirm the convergence of the extremum-seeking scheme if the persistency of excitation (PE) condition (7.116) is encountered. It remains fairly difficult to ensure that the dither signal employed is sufficiently rich. One of the main difficulties is that the calculation of the PE condition criteria depends on the value of the unknown parameters. In this study, we use the asymptotic value of the PE condition (7.116) to test whether a given dither signal is sufficiently exciting. The approach can be summarized as follows.

As $t \rightarrow \infty$, the analysis detailed above confirms that $\lim_{t\rightarrow\infty} z_s = 0$. This means that asymptotically, the substrate concentration S converges to $\frac{1}{\sqrt{\hat{\theta}_i}} + d(t)$. Since $\hat{\theta}_i$ converges to a constant value, the asymptotic dynamics of the substrate concentration, S_∞, coincide with the dynamics of the dither signal given (7.81) which converge to

$$\frac{dS_\infty}{dt} = \dot{d} = a(t) - k_d d(t) \tag{7.93}$$

as $t \rightarrow \infty$. The asymptotic dynamics of the production rate y_∞ are given by:

$$\begin{aligned}\frac{dy_\infty}{dt} = &\left(\frac{1-\theta_i S_\infty}{S_\infty\left(1+\theta_s S_\infty+\theta_i {S_\infty}^2\right)}\left(a(t)-k_d d(t)\right)\right.\\ &\left.+\frac{\theta_\mu S_\infty}{\left(1+\theta_s S_\infty+\theta_i {S_\infty}^2\right)}+\frac{1}{\left(S_0-S_\infty\right)}\left(a(t)-k_d d(t)\right)\right) y^\infty\\ &-\frac{\theta_k}{S_0-S_\infty}{y_\infty}^2.\end{aligned} \tag{7.94}$$

If we assume that a set of possible values of parameters θ_i, θ_μ and θ_s can be obtained, (7.93)-(7.94) can be solved for a given set of initial conditions and external signal $a(t)$. The corresponding trajectories are estimates of the asymptotic trajectories of the system subject to the extremum-seeking control. For each specific trajectory, we can calculate the corresponding value of the matrix:

$$\int_t^{t+T_0} \Psi_\infty(\tau)d\tau. \tag{7.95}$$

where $\Psi_\infty(t) = \Phi_a(S_\infty, y_\infty, u_\infty, \theta)\Phi_a(S_\infty, y_\infty, u_\infty, \theta)^T$ with $u_\infty = \frac{1}{(S_0 - S_\infty)}(\theta_k y_\infty + a(t) - k_d d(t))$:

$$\Phi_a\big(S_\infty, y_\infty, \theta, u_\infty\big) = \begin{bmatrix} -2\gamma_u {S_\infty}^2 - \gamma_u {S_\infty}^3 \theta_s - {S_\infty}^4 y_\infty \theta_\mu \\ -\gamma_u S_\infty + \gamma_u {S_\infty}^3 \theta_i - \theta_\mu {S_\infty}^3 y_\infty \\ {S_\infty}^2 y_\infty + \theta_s {S_\infty}^3 y_\infty + \theta_i {S_\infty}^4 y_\infty \end{bmatrix} \tag{7.96}$$

and $\gamma_u = (a(t) - k_d d(t)) y_\infty$.

The strategy for testing any specific dither signal consists of evaluating the minimum eigenvalue of matrix (7.95) over a specific time horizon. If the minimum eigenvalue is positive for all $t > 0$, the dither signal is deemed sufficiently rich and its use can be justified on the closed-loop extremum-seeking control system.

It is important to note that the corresponding conclusion depends entirely on the specific choice of parameter values that are used in the calculations. More work is required to investigate how this assessment can be conducted in a manner that is invariant of the choice of parameter values.

The use of this technique will be considered in the simulation study presented in the next section.

7.3.3. *Simulation results*

The aim of this section is to illustrate the performance of an adaptive extremum-seeking controller in a number of simulations, performed using a realistic example of a fed-batch process. The kinetic model parameters, yield coefficients and initial states used during numerical simulations are:

$$\begin{gathered} \mu_0 = 0.53\,\mathrm{h}^{-1},\ K_S = 1.2\,\text{g/l},\ K_I = 0.22\,\text{g/l},\ k_1 = 0.4,\ k_2 = 1 \\ X(0) = 7.2\,\text{g/l},\ S(0) = 2\,\text{g/l},\ S_0 = 20\,\text{g/l} \end{gathered} \tag{7.97}$$

For the Haldane model, from Figure 7.3, the maximum on the growth specific rate occurs at $S^* = \frac{1}{\sqrt{\theta_i}} = 0.52\,\text{g/l}$. The control objective is to design a controller for the dilution rate, u, to regulate substrate S at S^*. The controller requires online measurements of variables S and y, as well as the knowledge of the kinetic parameters, determining the S^*. These values are obtained using the estimation algorithm previously presented, using the measurements of y.

For the simulation study, we consider the following initial estimates of the kinetic parameters:

$$\hat{\theta}_\mu = 1,\ \hat{\theta}_S = 0.1,\ \hat{\theta}_I = 3\ \big(\hat{\mu}_0 = 10,\ \hat{K}_S = 10,\ \hat{K}_I = 0.03\big) \tag{7.98}$$

The design parameters for the extremum-seeking controller are set to:

$$\gamma_\mu = 10,\ \gamma_S = 200,\ \gamma_i = 200\ k_{y,0} = 20,\ k_z = 0.5,\ k_{d,0} = 1,\ \epsilon = 0.2$$

Dither signal $a(t)$ is chosen as follows:

$$\begin{aligned} a(t) = &\sum_{i=1}^{5} A_{1i} sin\big(\big(0.001 + (5 - 0.001)i/4\big)t\big) \\ &+ \sum_{i=1}^{5} A_{2i} cos\big(\big(0.01 + (5 - 0.01)i/4\big)t\big) \end{aligned} \tag{7.99}$$

where A_{1i} and A_{2i} are normally distributed random numbers in the interval $[-0.1, 0.1]$.

To test the richness of the dither signal, we calculate the smallest eigenvalue of matrix (7.95) over the interval $[0, 100]$ using the initial conditions, $x(0) = 7.2$, $s(0) = 1/\sqrt{3}$ and parameter estimates given by (7.98).

The simulation shows that the signal is sufficiently exciting in a region of these initial conditions and parameter values. The resulting dither signal was used in the subsequent simulation of the extremum-seeking control scheme. It should be noted that it is relatively easy in practice to provide a dither signal such that matrix (7.95) is positive definite. However, the convergence of the parameter estimates can also depend on the conditioning of this matrix. The calculations demonstrate that the condition number of the matrix remains around 10^3, a value that is relatively high. This indicates that parameter convergence may remain quite slow. In fact, a closer look at the spectral decomposition of this matrix indicates that the poor conditioning is associated with the adaptation of θ_s.

The convergence properties of the extremum-seeking control scheme are shown in Figure 7.4. We consider the initial conditions, $x(0) = 7.2$ and $s(0) = 2.0$. It is shown from Figure 7.4 that the extremum-seeking scheme converges to the intended growth rate value. The substrate concentration converges to the unknown optimum as well. The dilution rate manipulation resulting from the extremum-seeking control is also shown. The dilution rate is seen to reach its lower bound as a result of the dither signal, $a(t)$. Convergence of the kinetic parameters to their true values is achieved. It is important to note that the control performance is strongly dependent on the convergence of parameter θ_I, determining the set point for the control law, as illustrated by the substrate evolution, from Figure 7.4. Overall, extremum-seeking is shown to perform satisfactorily for this case.

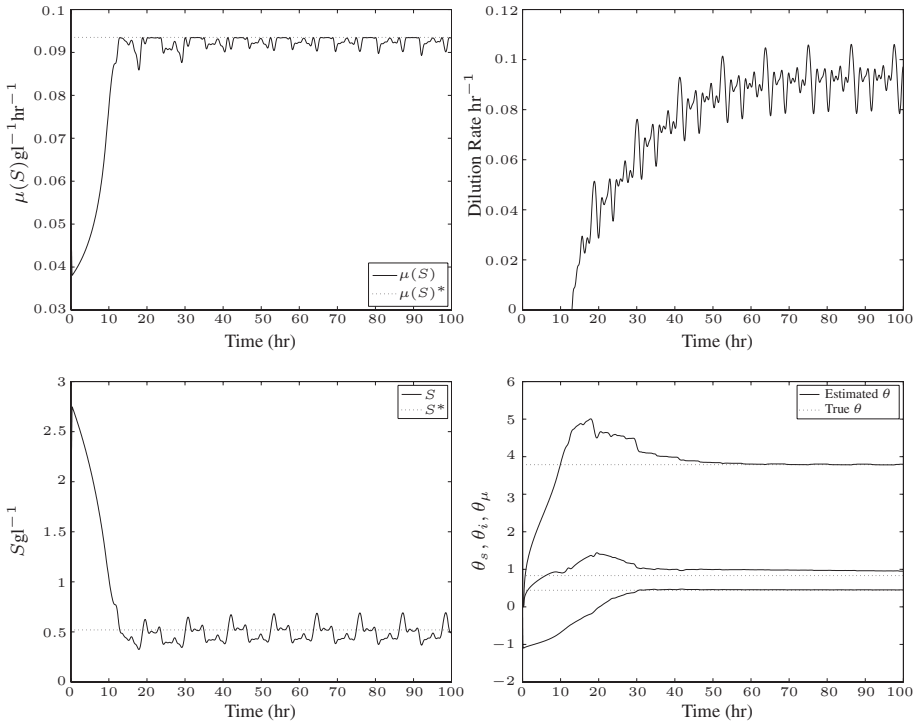

Figure 7.4. *Illustration of the convergence properties*

In Krstic *et al.*, an extremum-seeking scheme was proposed to optimize the production rate for a class of bioreactors governed by Monod kinetics and Haldane kinetics [WAN 99]. An extremum-seeking control was developed following the design procedure proposed in [WAN 99]. The main difference is that we use the procedure to optimize the growth rate $\mu(S)$. In this case, the extremum-seeking scheme yields the closed-loop system:

$$\begin{aligned}
\dot{x} &= (\mu - D)x \\
\dot{S} &= -k_1 \mu x + (S_0 - S)D \\
\dot{\hat{D}} &= k(\mu - \eta) + a\sin(\omega t) \\
\dot{\eta} &= \omega_h(\mu - \eta) \\
D &= \hat{D} + a\sin(\omega t)
\end{aligned} \tag{7.100}$$

where μ is given by (7.56). Note that the structure assumes that the actual value of μ is measured in this case. This is extremely unlikely since this would require detailed structural information about the parameter values of $\mu_{\max}$, K_s and K_i entering the expression for μ.

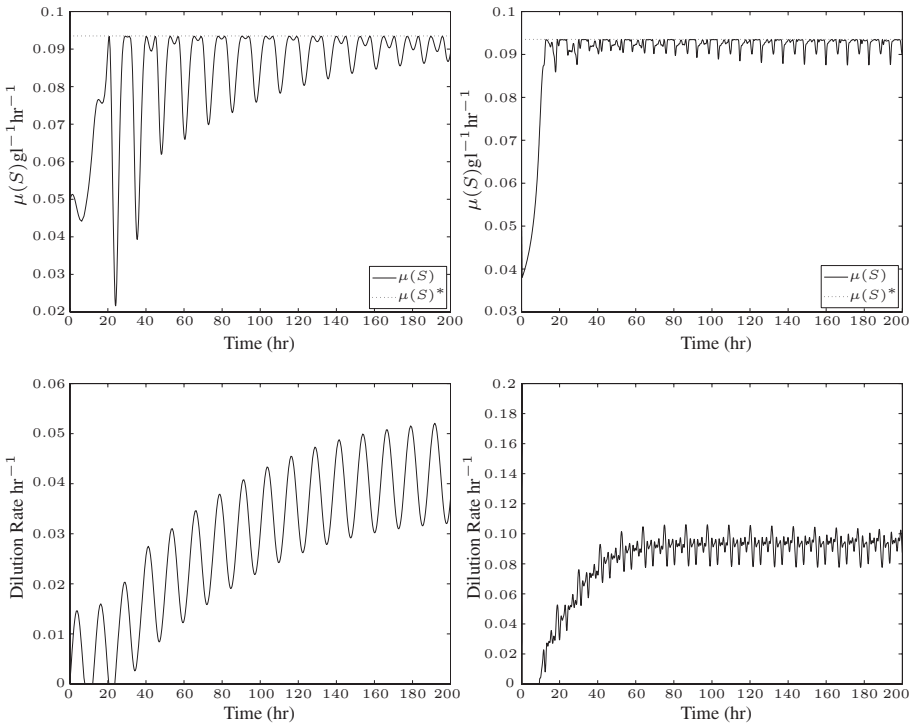

Figure 7.5. *Performance of the proposed scheme (right) and the controller proposed in [WAN 99] for the case* $x(0) = 7.2$, $s(0) = 2.0$

In order to facilitate the comparison, the tuning parameters of the extremum-seeking scheme are set to the following values:

$$a = 0.01, \quad \omega = 0.75, \quad k = 5, \quad \omega_h = 0.1$$

The tuning parameters were assigned following the guidelines outlined in [KRS 00a]. Two simulations were performed. The first simulation was initiated at $X(0) = 7.2$, $S(0) = 2.0$, as above. Figure 7.5 shows the comparison between the performance of the two extremum-seeking schemes. On the left hand side, we show the dilution rate and specific growth rate μ for the proposed extremum-seeking controller. On the right side, we show the dilution rate and specific growth rate resulting from the application of the extremum-seeking scheme proposed in [WAN 99]. The results demonstrate that the two control schemes provide comparatively equivalent convergence properties. The scheme of [WAN 99] provides a slower convergence which could be improved by further adjustments of the design parameters. The values employed were the values that were found to provide the best performance for this system.

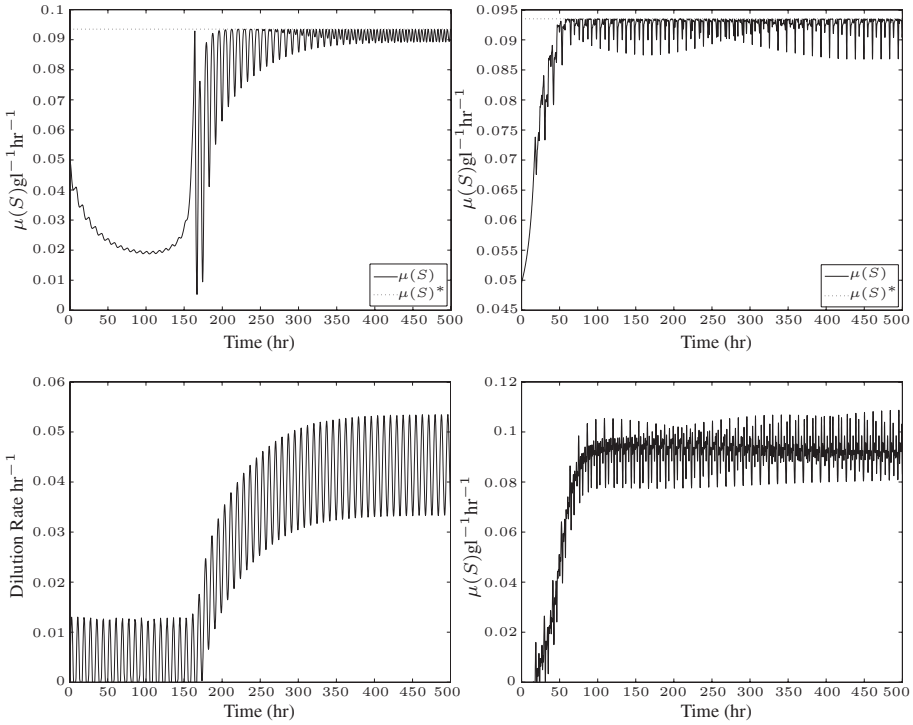

Figure 7.6. *Performance of the proposed scheme (right) and the controller proposed in [WAN 99] for the case* $x(0) = 1.2$*,* $s(0) = 2.0$

In the second simulation, the initial concentration of biomass was set to $X(0) = 1.2$. The simulation results are shown in Figure 7.6. As above, we show the dilution rate and specific growth rate for the proposed scheme on the right hand side and the results for the controller proposed by [WAN 99] on the left hand side. The scheme proposed in [WAN 99] provides very poor convergence properties compared to the scheme proposed here.

Overall, the results indicate that the proposed scheme provides very consistent performance for this system.

In the next set of simulations, we wish to illustrate the controller performance for regulation (as illustrated in Figure 7.7) by introducing a disturbance in the S_0 concentration between 60 and 70 hours. As expected, the controller quickly rejects the disturbance while attenuating its effect on S which is accurately regulated at the set point during the whole operation.

The last simulation illustrates the performance of the extremum-seeking controller in the presence of noisy measurements. As in the previous case, we consider the

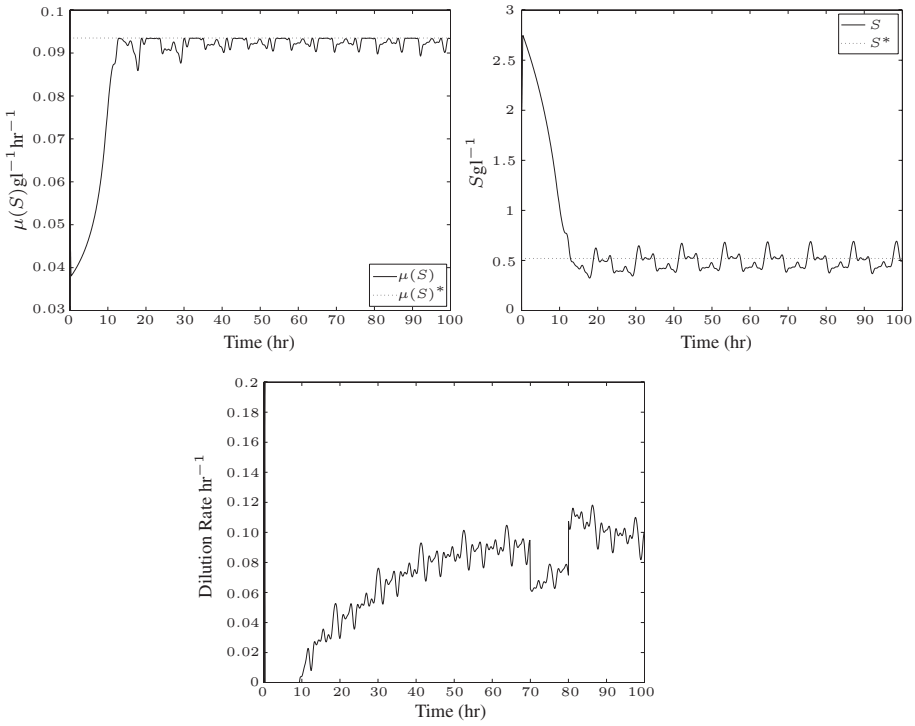

Figure 7.7. *Illustration of the robustness properties.* S_0 *is changed from* 20 *g/l to* 40 *g/l from* $t = 60$ *hr to* $t = 70$ *hr*

operation of the bioreactor in the presence of a step in inlet substrate concentration, S_0 from 20 g/l to 40 g/l from $t = 60$ hr to $t = 70$ hr. In addition, it is assumed that the substrate measurement, S, and the production rate measurements, y, are corrupted by additive measurement noise. The measured substrate concentration is given by $S_m = S + 0.1n_S$ where n_S is a unit variance normally distributed additive noise term. Similarly, the measured production rate is given by, $y_m = y + 0.005n_y$, where n_y is a unit variance normally distributed additive noise term.

The results of the simulation are given in Figure 7.8. The results demonstrate that the extremum-seeking controller performs adequately in the presence of measurement noise.

7.4. Appendix: analysis of the parameter convergence

By LaSalle's invariance principle, the error vector $(z_s, e_y, \tilde{\theta})$ converges to the largest invariant set M of dynamic system (7.66) and (7.85)–(7.87) contained in the